

February 2010

Master's Thesis

A Study on Weldability of  
TIG Assisted Friction Stir  
Dissimilar Welding of  
Al6061 Alloy and STS Sheet

Graduate School of Chosun University

Department of Naval Architecture and  
Ocean Engineering

Geun-Hong Jeon



# A Study on Weldability of TIG Assisted Friction Stir Dissimilar Welding of Al6061 Alloy and STS Sheet

TIG-FSW Hybrid 용접기술을 이용한 이종재료  
Al6061 Alloy - STS 용접부의 용접성에 관한 고찰

February 2010

Graduate School of Chosun University

Department of Naval Architecture and  
Ocean Engineering

Geun-Hong Jeon

# A Study on Weldability of TIG Assisted Friction Stir Dissimilar Welding of Al6061 Alloy and STS Sheet

Advisor : Professor Han-Sur Bang

A Thesis submitted for the degree of  
Master of Engineering

October 2009

Graduate School of Chosun University

Department of Naval Architecture and  
Ocean Engineering

Geun-Hong Jeon

# 全根弘의 碩士學位論文을 認准함

委員長 朝鮮大學校 教授 房 熙 善 印

委 員 朝鮮大學校 教授 房 漢 瑞 印

委 員 朝鮮大學校 教授 權 寧 燮 印

2009年 11月

朝鮮大學校 大學院

# CONTENTS

List of Table .....	III
List of Figures .....	IV
Abstract .....	V

## Chapter 1. Introduction

1 . 1 Background & Purpose .....	1
----------------------------------	---

## Chapter 2. Theoretical background

2 . 1 Principles and characteristics of FSW .....	2
2 . 2 Principles and characteristics of GTAW .....	5
2 . 3 Type and characteristics of aluminum alloy .....	7
2 . 4 Type and characteristics of stainless steel .....	11

## Chapter 3. Experiment method of TIG–FSW process

3 . 1 Experimental work for TIG–FSW .....	14
3.1.1 TIG–FSW equipment and experimental setup ....	14
3.1.2 Details of objective materials .....	16
3 . 2 Description of tool material .....	18
3 . 3 TIG assisted Friction stir welding condition .....	20
3 . 4 Experiment method .....	23
3.4.1 Tensile test .....	23
3.4.2 Hardness test .....	24

3.4.3 Bending test .....	25
3.4.4 Micro structure analyses .....	26
Chapter 4. Experimental Investigation & Results	
4 . 1 Welding condition and bead shape .....	27
4.1.1 Experiment by TIG Welding .....	27
4.1.2 Experiment by Friction Stir Welding .....	28
4.1.3 Experiment by TIG assisted Friction Stir Welding .....	31
4 . 2 Tensile test results .....	37
4.2.1 Tensile test of similar joint (Al6061–T6) .....	37
4.2.2 Tensile test of FSW dissimilar joint .....	38
4.2.3 Tensile test of TIG assisted FSW dissimilar joint .....	41
4 . 3 Hardness test results .....	47
4 . 4 Bending test results .....	49
4 . 5 Micro structure analyses of dissimilar joint .....	51
4.5.1 Micro structure of FSW dissimilar joint .....	51
4.5.2 Micro structure of TIG assisted FSW dissimilar joint .....	51
4.5.3 Microstructure analyses by using SEM and EDS.....	54
Chapter 5. Conclusion .....	58
Reference .....	60

## List of Tables

Table 2.1	Typical property for aluminium .....	8
Table 3.1	Chemical composition and mechanical property .....	17
Table 3.2	Tungsten carbide specifications and tool surface coating ·	18
Table 3.3	TIG Welding condition .....	21
Table 3.4	TIG-FSWelding condition .....	21
Table 4.1	TIG welding parameters and obtained bead shapes .....	27
Table 4.2	FSW parameters and obtained bead shapes .....	29
Table 4.3	TIG assisted FSW parameters and obtained bead shapes·	32
Table 4.4	Bead appearance of similar joint specimen considered for tensile test .....	37
Table 4.5	Cross sections and fractured specimens of dissimilar joint by FSW .....	39
Table 4.6	Stress-strain curve for dissimilar weld joint by FSW ....	40
Table 4.7	Cross sections and fractured specimens of dissimilar joint TIG assisted FSW .....	42
Table 4.8	Stress-strain curve for dissimilar weld joint by TIG assisted FSW .....	44
Table 4.9	Bending test result .....	50



# List of Figures

Fig. 2.1	Schematic of friction stir welding .....	3
Fig. 2.2	Microstructural regions in FSWelded Al alloys .....	3
Fig. 2.3	Schematic of GTAWelding .....	5
Fig. 2.4	Division of aluminum .....	8
Fig. 2.5	Families of stainless steels .....	12
Fig. 2.6	The austenitic stainless steel .....	12
Fig. 3.1	WINXEN FSW equipment details .....	15
Fig. 3.2	Setup for TIG-FSW process .....	15
Fig. 3.3	Configuration of specimen .....	17
Fig. 3.4	Tool dimensions .....	19
Fig. 3.5	Tool shape .....	19
Fig. 3.6	Schematic of TIG assisted FSWelding process .....	22
Fig. 3.7	Welding configuration for TIG-FSW .....	22
Fig. 3.8	Tensile test specimen dimensions .....	23
Fig. 3.9	Vickers hardness test machine and specimen .....	24
Fig. 3.10	Schematic of bending test fixture and bending test specimen size dimension .....	25
Fig. 3.11	Optical microscope .....	26
Fig. 4.1	Tested specimen and Stress-Strain curve .....	37
Fig. 4.2	Tensile test result of welded specimen .....	46
Fig. 4.3	Hardness distribution of dissimilar(TIG assisted FSW) .....	48
Fig. 4.4	Microstructural(FSW) .....	52
Fig. 4.5	Microstructural(TIG assisted FSW) .....	53
Fig. 4.6	SEM micrograph of dissimilar weld .....	55
Fig. 4.7	SEM of dissimilar weld tensile fracture surface .....	56
Fig. 4.9	EDS analysis of dissimilar weld .....	57

# ABSTRACT

## TIG-FSW Hybrid 용접기술을 이용한 이종재료 Al6061 Alloy - STS304 용접부의 용접성에 관한 고찰

Jeon, Geun-hong

Advisor : Prof. Bang, Han-sur, Ph.D.

Department of Naval Architecture and  
Ocean Engineering ,

Graduate School of Chosun University

최근, 각종 산업분야에 있어서 경량화 구조가 증가하고 있으며 특히 수송 기계분야(철도차량, 자동차, 선박, 항공기 등)에 있어서 경량화에 의한 연비 절감 및 지구 환경보호와 에너지 절감에 대한 요구가 높아짐에 따라 경량 부재의 적용이 빠른 속도로 확대되고 있다.

1981년 영국의 용접연구소(TWI)에서는 비 용융 접합공정인 Friction stir welding(FSW:마찰교반접합) 방법을 개발하였다. FSW기술은 마찰용접에서 유래되어 용접에 의한 변형이 적고 용접결함, 흠, 유해광선의 발생 없이 우수한 품질의 접합부를 얻을 수 있으며, 기계적 특성 또한 우수한 접합 방법이다. 경량금속(Al, Mg, Cu합금 등)은 기존 용융용접에서 문제시 되고 있는 응고균열, 기공, 산화 등의 결함을 최소화 할 수 있는 고상접합공정인 Friction stir welding이 다양한 산업분야에서 크게 주목받고 있으며 이미 적용되어지고 있다. 접합대상이 기존의 알루미늄과 알루미늄 동종계의 경량합금에서 이종재의 경량합금의 접합 영역 뿐 아니라 경합금과 철강 재료의 접합의 영역까지 확대 되고 있다. 모든 구조물을 지지하는 부분의 부재는 강도가 뛰어난 부재를 사용하여야 하므로 경량합금과 철계 합금의 이종접합이 필연 시 되고 있다. FSW를 이용하여 이종재료를 접합할 경우 물리적인 성질이 상이하여 기존 동종재료의 FSW접합 방식으로는 건전한 접합부를 쉽게 얻을 수 없어 두 재료 중 연질인 재료에 마찰교반접합 Tool을 삽입하여 건전한 접합부를 얻은 결과가 보고된바 있으나 아직은 연구가 많이 미흡한 실정이다.

따라서 본 연구는 비강도가 우수한 알루미늄 합금과 우수한 부식특성 높은 강도를 나타내는 스테인리스강의 이종재료를 FSW와 TIG welding을 결합한 하이브리드 용접을 수행함으로써 접합부의 미세조직 및 기계적 강도를 측정하고 접합특성을 파악하여 선박, 자동차 및 항공기, 수송기계 부품제작에 적용 가능성을 고찰하고자 한다.

# Chapter 1

## INTRODUCTION

### 1.1 Background & Purpose

There has been a sharp rise in production efficiency by highly industrialized, fuel savings caused by lightweight technology and the demand for the lightweight metal to comply with the regulations of environmental pollution. A environmental friendly welding process become seriously considered, whit this, joining process of lightweight alloy has played a prominent role in the industrial technique as well. More than anything else, FSW which makes a conspicuous figure is more environmental friendly then existing welding process, and its low welding deformation and excellent strength in the aspect of welded structure has already been given proof from various research. The use of FSW is becoming widespread and joining object expands its area of use from existing similar system of magnesium and aluminum to a joining area of dissimilar light weight alloys. So does in a joining area of light alloys and steel material. The case of joining a dissimilar plate using FSW has been known that is not easily obtained because of different physical properties in the way of FSW joining method of using existing similar materials.

This research found that aluminum, which has high strength to weight and stainless steel, which has excellent corrosion properties and high strength, can be joined by FSW and TIG Welding. After above Hybrid Welding, we will search the characteristics of joining by measuring the microstructure and mechanical strength at copula.

Consequently, the purpose of the research is to investigate the possibility of application of FSW and TIG Welding in the field of vessels, automobile, aircraft and the parts of transportation machinery.

## Chapter 2

# THEORETICAL BACKGROUND

### 2.1 Principles and characteristics of FSW

#### 2.1.1 Principles of FSW

Friction Stir Welding is a solid state joining method with five phases of actions in its entire process(Fig. 2.1). The first is the plunging period, where the pin is fully and shoulder is partially plunged into the joint line of the work piece. The second action is in the dwell period during which the tool keeps on rotating at the plunge point. In this phase the material around the tool is heated due to the friction between the probe and matrix surfaces due to sliding action. Due to this thermo-mechanical action, materials around the tool get plasticized. The third phase of action is in the steady state welding period, during which the rotating tool is traversed along the welding line. This is followed by a second dwell period, which is the fourth phase of action. The last and the fifth phase of action is in the releasing period during which the rotating tool is raised up from the weld line leaving behind a pin cavity in the work piece.

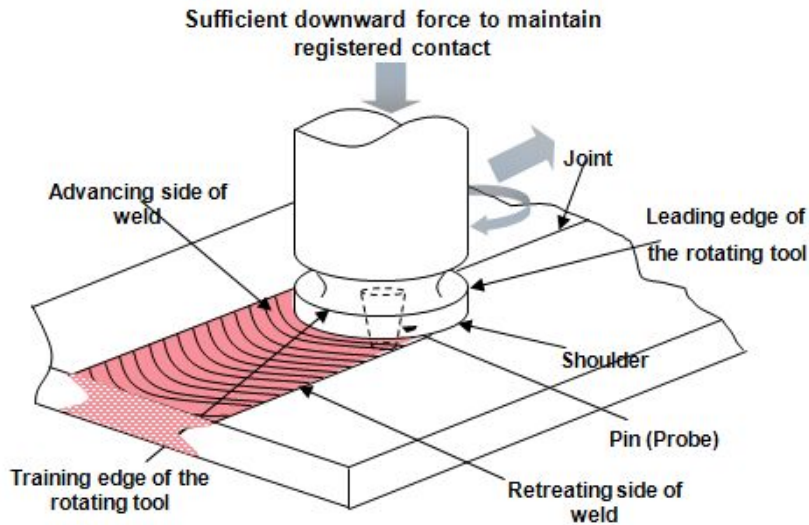
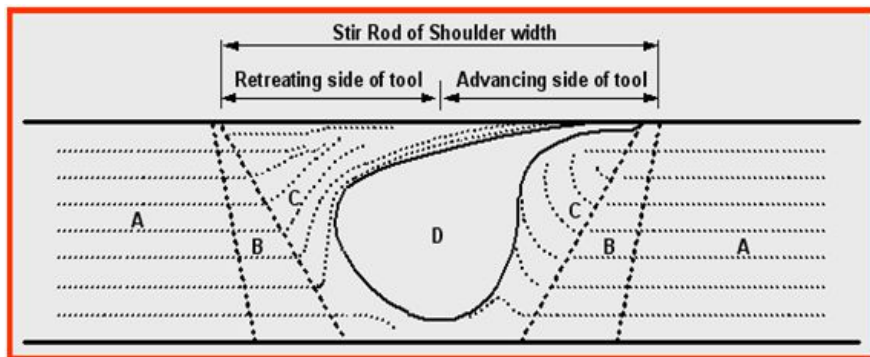


Fig. 2.1 Schematic of Friction Stir Welding



- A: BM (Base Metal)
- B: HAZ (Heat Affected Zone; affected by heat generated during FSW )
- C: TMAZ (Thermomechanically Affected Zone; contains material that interacts indirectly with the tool , plastically deformed with partial recrystallization)
- D: SZ (Stir Zone; contains material that interacts directly with the tool, dynamically recrystallized)

Fig. 2.2 Microstructural regions in FSWelded Al alloys

## 2.1.2 Characteristics of FSW

### 1) Advantages of Friction stir welding

- Good mechanical properties in the as welded condition Improved safety due to the absence of toxic fumes or the spatter of molten material.
- No consumables – conventional steel tools[clarification needed] can weld over 1000m of aluminium and no filler or gas shield is required for aluminium.
- Easily automated on simple milling machines – lower setup costs and less training.
- Can operate in all positions (horizontal, vertical, etc), as there is no weld pool.
- Generally good weld appearance and minimal thickness under/over –matching, thus reducing the need for expensive machining after welding.
- Low environmental impact.

### 2) Disadvantages of Friction stir welding

- Exit hole left when tool is withdrawn.
- Large down forces required with heavy-duty clamping necessary to hold the plates together.
- Less flexible than manual and arc processes (difficulties with thickness variations and non-linear welds).
- Often slower traverse rate than some fusion welding techniques although this may be offset if fewer welding passes are required.

## 2.2 Principles and characteristics of GTAW

### 2.2.1 Principles of GTAW

Gas Tungsten Arc Welding (GTAW) is frequently referred to as TIG welding. TIG welding is a commonly used high quality welding process (Fig. 2.3). TIG welding has become a popular choice of welding processes when high quality, precision welding is required. In TIG welding an arc is formed between a nonconsumable tungsten electrode and the metal being welded. Gas is fed through the torch to shield the electrode and molten weld pool. If filler wire is used, it is added to the weld pool separately. In the TIG process the arc is formed between a pointed tungsten electrode and the workpiece in an inert atmosphere of argon or helium. The small intense arc provided by the pointed electrode is ideal for high quality and precision welding. Because the electrode is not consumed during welding, the welder does not have to balance the heat input from the arc as the metal is deposited from the melting electrode. When filler metal is required, it must be added separately to the weldpool.

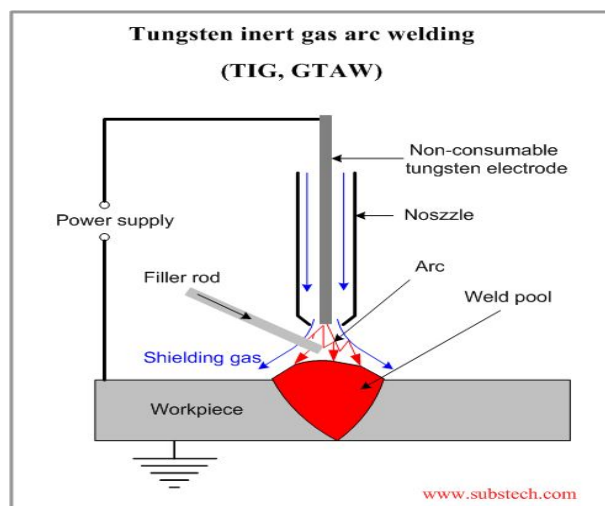


Fig. 2.3 Schematic of GTAWelding



## 2.2.2 Characteristics of GTAW

### 1) Advantages of TIG Welding

- Precise control of welding variables (heat).
- Welds can be made with or without filler metal.
- Weld composition is close to that of the parent metal.
- High quality weld structure.
- Slag removal is not required (no slag).
- Thermal distortions of work pieces are minimal due to concentration of heat in small zone.

### 2) Disadvantages of TIG Welding

- Excessive electrode consumption.
- Arc wandering.
- Oxidized weld deposit.
- Difficult arc starting.
- Low welding rate.
- Relatively expensive.
- Requires high level of operators skill.

### 3) Shielding Gases

- Argon.
- Argon/Helium.
- Oxidized weld deposit.

## 2.3 Type and characteristics of aluminum alloy

### 2.3.1 Type of aluminum alloys

Aluminium alloys are alloys in which aluminium is the predominant metal. Typical alloying elements are copper, zinc, manganese, silicon, and magnesium. There are two principal classifications, namely casting alloys and wrought alloys, both of which are further subdivided into the categories heat-treatable and non-heat-treatable (Fig. 2.4).

Cast aluminium alloys yield cost effective products of low melting point, although they generally have lower tensile strengths than wrought alloys. The most important cast aluminium alloy system is Al-Si, where the high levels of silicon (4–13%) contribute effective good casting characteristics.

Wrought alloys are divided into two classes—nonheat treatable and heat treatable. In the nonheat-treatable class, strain hardening (cold-working) is the only means of increasing the tensile strength. Heat-treatable alloys may be hardened by heat treatment, by cold-working, or by the application of both processes.

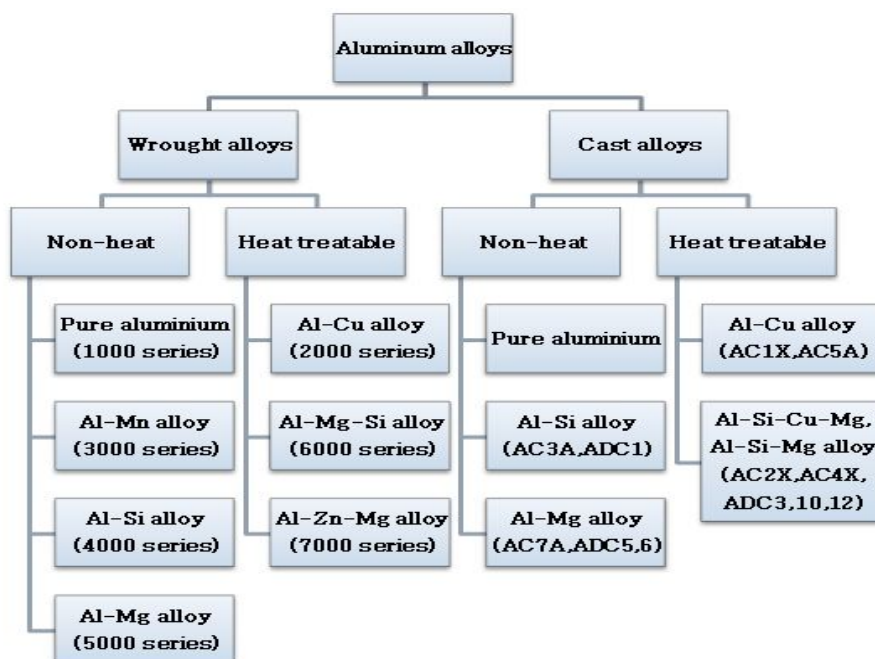


Fig. 2.4 Division of Aluminum

Table 2.1 Typical properties for aluminium

Property	Value
Atomic Number	13
Atomic Weight (g/mol)	26.98
Valency	3
Crystal Structure	Face centred cubic
Melting Point (°C)	660.2
Boiling Point (°C)	2480
Mean Specific Heat (0-100°C) (cal/g.°C)	0.219
Thermal Conductivity (0-100°C) (cal/cms. °C)	0.57
Co-Efficient of Linear Expansion (0-100°C) (x10 <sup>-6</sup> /°C)	23.5
Electrical Resistivity at 20°C (μΩcm)	2.69
Density (g/cm <sup>3</sup> )	2.6898
Modulus of Elasticity (GPa)	68.3
Poisson's Ratio	0.34

## 2.3.2 Characteristics of aluminum alloy 6061

Al 6061 is a precipitation hardening aluminum alloy, containing magnesium and silicon as its major alloying elements. It has good mechanical properties and exhibits good weldability. It is one of the most common alloys of aluminum for general purpose use.

It is commonly available in pre-tempered grades such as, 6061-O (solutionized), 6061-T6 (solutionized and artificially aged), 6061-T651 (solutionized, stress-relieved stretched and artificially aged).

### 1) Mechanical properties

The mechanical properties of 6061 depend greatly on the temper, or heat treatment, of the material.

- 6061-O

Annealed 6061 (6061-O temper) has maximum tensile strength no more than 18,000 psi (125 MPa), and maximum yield strength no more than 8,000 psi (55 MPa). The material has elongation (stretch before ultimate failure) of 25–30 %.

- 6061-T4

T4 temper 6061 has an ultimate tensile strength of at least 30,000 psi (207 MPa) and yield strength of at least 16,000 psi (110 MPa). It has elongation of 16%.

- 6061-T6

T6 temper 6061 has an ultimate tensile strength of at least 42,000 psi (290 MPa) and yield strength of at least 35,000 psi (241 MPa). In thicknesses of 0.250 inch (6.35 mm) or less, it has elongation of 8% or more; in thicker sections, it has elongation of 10%. T651 temper has similar mechanical properties.

## 2) Application

- 6061 is widely used for construction of aircraft structures, such as wings and fuselages, more commonly in homebuild aircraft than commercial or military aircraft.
- 6061 is used for yacht construction, including small utility boats.
- 6061 is commonly used in the construction of bicycle frames and components.
- 6061 is also used in automotive parts, such as wheel spacers.
- 6061 is also used in the manufacture of aluminum cans for the packaging of foodstuffs and beverages.

## 2.4 Type and characteristics of stainless steel

### 2.4.1 Types of stainless steel

Stainless steel is defined as a steel alloy with a minimum of 10.5 or 11% chromium content by mass. All stainless steels can be grouped into three metallurgical classes a)Austenitic b)Ferritic and c)Martensitic based on their microstructure. Each of the classes has different welding requirements. Fig. 2.5 shows the families of stainless steels according to Ni–Cr content.

**Austenitic stainless steels** contain at least 16% chromium and 6% nickel(the basic grade 304 is sometimes referred to as 18/8) and range through to the high alloy or "super austenitics"such as 904L and 6% molybdenum grades. Additional elements can be added such as molybdenum, titanium or copper, to modify or improve their properties, making them suitable for many critical applications involving high temperature as well as corrosion resistance. The different grade of Austenitic stainless steels is shown in Fig. 2.6.

**Ferritic stainless steels** are plain chromium ( $10\frac{1}{2}$  to 18%) grades such as Grade 430 and 409. Their moderate corrosion resistance and poor fabrication properties are improved in the higher alloyed grades such as 434 and 444.

**Martensitic stainless steels** are also based on the addition of chromium as the major alloying element but with a higher carbon and generally lower chromium content (eg:12% in Grades 410 and 416) than the ferritic types; Grade 431 has a chromium content of about 16%, but the microstructure is still martensite despite this high chromium level because this grade also contains 2% nickel.

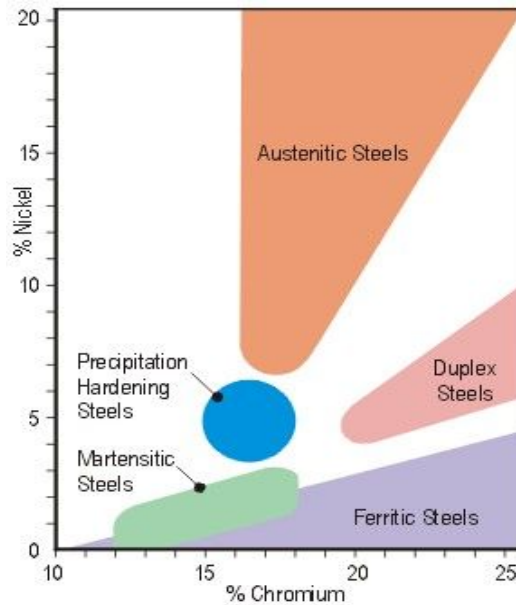


Fig. 2.5 Families of stainless steels

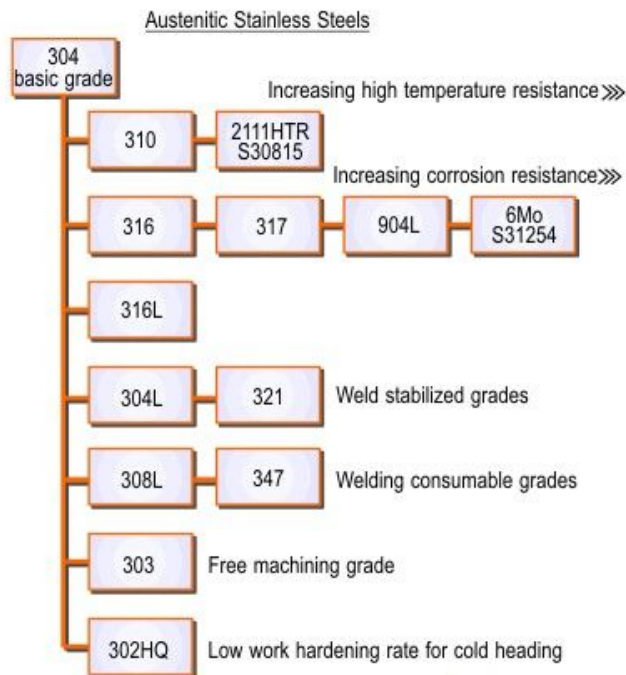


Fig. 2.6 The austenitic stainless steels

## 2.4.2 Characteristics of stainless steel 304

Type 304 is a variation of the basic 18–8 grade, Type 302, with a higher chromium and lower carbon content. Lower carbon minimizes chromium carbide precipitation due to welding and its susceptibility to intergranular corrosion. In many instances, it can be used in the "as-welded" condition.

### 1) Characteristics of STS304

- Forming and welding properties.
- Corrosion/ oxidation resistance thanks to the chromium content.
- Deep drawing quality.
- Excellent toughness, even down to cryogenic temperatures which are defined as very low temperatures.
- Low temperature properties responding well to hardening by cold working.
- Ease of cleaning, ease of fabrication, beauty of appearance.

### 2) Application of STS304

- Applied largely in automotive, shipbuilding/marine, railway, aerospace industries.
- Applied for tanks and containers for a large variety of liquids and solids.
- Architectural panelling, railings & trim.
- Chemical containers, including for transport.
- Heat Exchangers.
- Woven or welded screens for mining, quarrying & water filtration.
- Dyeing industry.
- Also highly suitable and applied in dairy equipment such as milking machines, containers, homogenizers, sterilizers, and storage and hauling tanks, including piping, valves, milk trucks and railroad cars.



# Chapter 3

## EXPERIMENT METHOD OF TIG–FSW PROCESS

### 3.1 Experimental work for TIG–FSW

#### 3.1.1 TIG–FSW equipment and experimental setup

WINXEN FSW system together with DAIHEN Inverter ELECON 500P TIG welding machine is used in this welding experiment. FSW Tool system combined with TIG torch was arranged in order to conduct the welding experiment in X, Y and Z directions. Heat treated STD 11 plate was replaced with mild steel backing plate in order to prevent the backing plate wear.

Fig. 3.1 shows the TIG assisted FSW equipment.

TIG welding torch to preheat the stainless steel material was attached adjacent to the FSW tool shoulder, inclined at 60degrees. The electrode tip of TIG is placed at a distance of about 15mm from the FSW tool shoulder. When the TIG torch is placed near to the tool shoulder, ie, less than 15mm, the current affects the tool surface and thus the desired preheating is not achieved.

Fig. 3.2 shows the experimental setup for TIG assisted FSW.

ITEMS		RANGE
TYPE		GANTRY TYPE
Welding Speed	X-axis	0.5~10 mm/sec
	Y-axis	0.5~10 mm/sec
	Z-axis	0.5~10 mm/sec
	R-axis	1~20 RPM
Rotation		300~3000 RPM
LOAD Capacity		Max. 3000Kgf



Fig. 3.1 WINXEN FSW equipment details

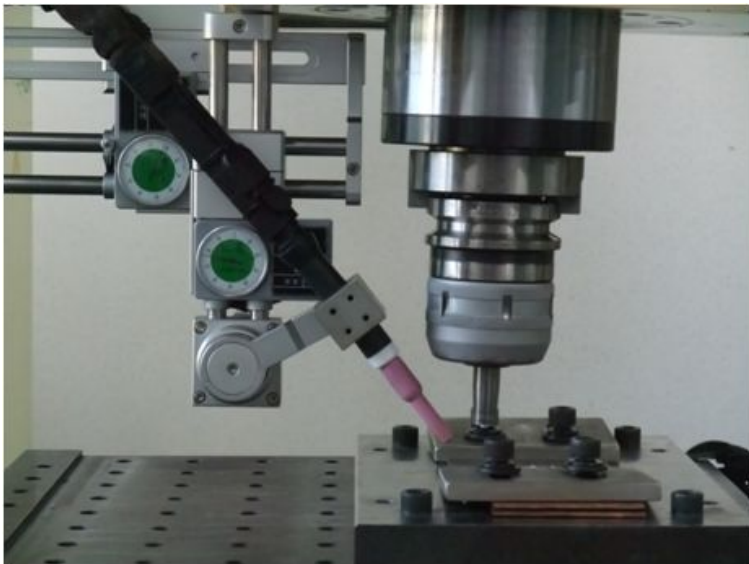


Fig. 3.2 Setup for TIG-FSW process

### 3.1.2 Details of objective materials

The chemical compositions and mechanical properties of the materials used in the experiment are given at Table 3.1. Specimens of size 200mm(L)  $\times$  100mm(W)  $\times$  3mm(T) were made and the edge preparation at the contact side of the specimens is done by milling process. The welding surface was wiped with Methyl Alcohol to remove the grease before welding process. Fig 3.3 were shown a plot plan of specimen. Fig. 3.3 shows the configuration of the weld specimen.

Table 3.1 Chemical composition and mechanical property

Material	Chemical composition (wt%)								
Al6061 -T6	Al	Fe	Si	Cr	Mg	Ti	Cu	Mn	Zn
	98	0.7	0.4-0.8	0.04-0.35	0.1	0.03	0.15-0.4	0.15	0.25
	Mechanical properties								
	Yield stress (MPa)	Elongation (%)	Tensile stress (MPa)	Heat conduction coeff.	Density (g/cc)	Melting Point			
	276	12	310	0.4	2.7	650			
Material	Chemical composition (wt%)								
STS 304	C	Si	Mn	P	S	Ni	Cr	Mo	기타
	0.08	1.00	2.00	0.040	0.030	8.0~10.50	18.0~20.0	-	-
	Mechanical properties								
	Yield stress (MPa)	Elongation (%)	Tensile stress (MPa)	Heat conduction coeff.	Density (g/cc)	Melting Point			
	265	55	628	0.039	7.94	1450			

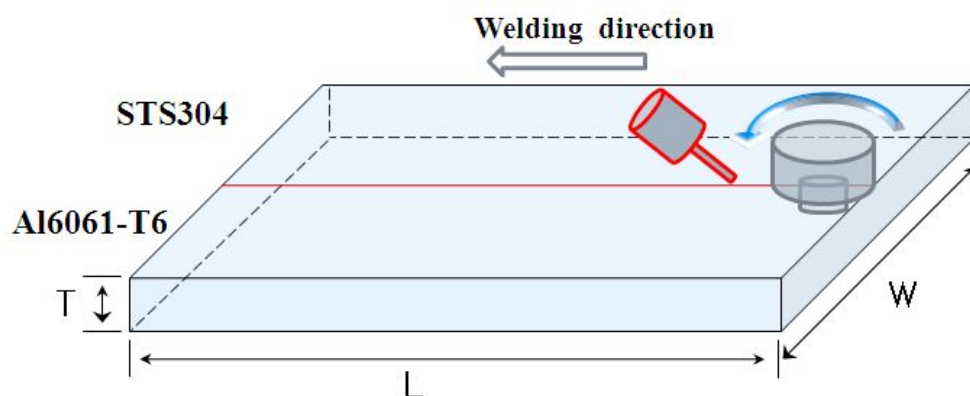


Fig. 3.3 Configuration of weld specimen

## 3.2 Description of tool material

The tool material is made of 12%Co tungsten carbide (WF20) to prevent the tool wear due to frictional contact with stainless steel plate while conducting FSW process.

The tool is shaped on diamond grinding machine and surface nano coating(AlTiN/Si3N4) is done to improve wear resistance, frictional resistance, high temperature hardness, hardness and machinability.

Table 3.2 shows the detail of tungsten carbide rod specifications and tool surface coating used for tool making.

Tool pin shape is of smooth frustum type and shoulder is designed to obtain the proper mixing at the stir zone with good plastic flow of the material. The shoulder is made concave with 3° clearance to act as an escape volume for the material displaced by the probe during the plunge action. The dimensions of shoulder and probe to cause substantial improvements in productivity and quality is shown in Fig 3.4 and tool shape is shown in Fig 3.5.

**Table 3.2 Tungsten carbide rod specifications and Tool surface coating**

(a) Tungsten carbide rod specifications

Co( $\pm 0.5\%$ )	Grade	WC( $\pm 0.5\%$ )	Grain Size( $\mu\text{m}$ )	Density (g/cc)	Hardness (HV30)
12%	WF20	88%	0.6	14.15	1670

(b) Tool surface coating

Grade	Coefficient of friction	Fine Hardness (Gpa)	Maximum temperature( $^{\circ}\text{C}$ )	Applications
AlTiN / Si3N4	0.45	45	1200	<ul style="list-style-type: none"> <li>◆ High efficiency nano structure and nano hardness</li> <li>◆ Ultra Heat resistances</li> <li>◆ High efficiency at dry high speed condition</li> </ul>

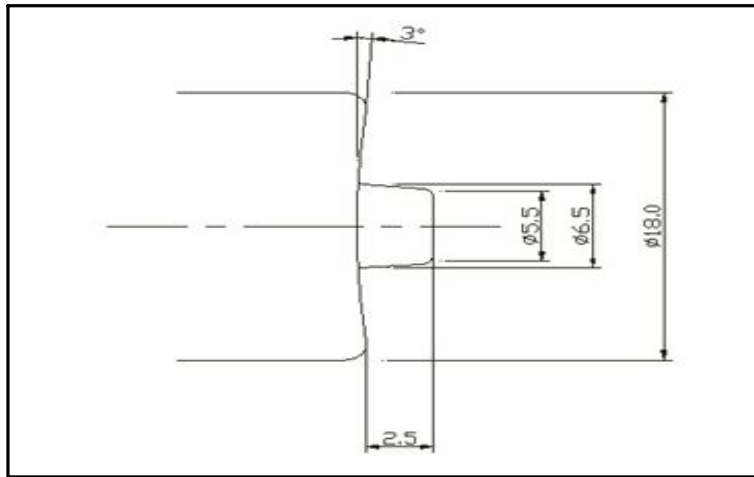


Fig. 3.4 Tool dimensions



Fig. 3.5 Tool shape

### 3.3 TIG assisted Friction stir welding condition

To ensure a successful and efficient welding cycle of dissimilar welding by TIG assisted FSW, the important parameters to be considered are tool rotating speed, tool travel speed, tool rotating direction and tool plunge position. The parameters to be considered for TIG heat source to obtain the desired preheating are current, shielding gas torch angle and FSW tool – TIG torch spacing.

The TIG preheating conditions was obtained by conducting BOP tests on STS304 plate and is given in Table 3.3.

From the previous researches on FSW of dissimilar materials, it is relevant that it is impossible to join dissimilar plates with tool position at the welding center line. This is due to the difference in hardness and mechanical properties of the materials.

Moreover, when tool was placed at the centre weld line, more heat is generated with high frictional force on STS304 side producing tool wear. Therefore, the plunge position was kept such that the probe outer face is at a distance 1–1.5mm away from the weld centre line to STS304 side and remaining part of the tool plunges at Al6061–T6 side.

The actual welding process was carried out with tool rotating direction counter clock wise (ccw) placing STS304 in the advancing side and Al6061–T6 in the retreating side. The TIG electrode was placed at 2mm away from weld center line to STS304 side and 15mm from the shoulder face. Fig. 3.6 shows the Schematic of TIG assisted FSWelding process. Welding condition for TIG assisted FSWelding process is given in Table 3.4. Fig. 3.7 shows the position of materials, TIG electrode and plunging of tool for TIG–FSW.

Table 3.3 TIG Welding condition



Shield Gas : Ar - 5ℓ/min, wire : Φ 1.6mm				
No.	Current	Pulsed Current	Welding speed	Torch angle
1	140A	40A	2mm/s	40°
Macro				Width :4mm Depth : 2.2mm
Shield Gas : Ar - 10ℓ/min, wire : Φ 2.4mm				
No.	Current	Pulsed Current	Welding speed	Torch angle
2	70A	70A	1mm/s	60°
Macro				Width :1.5mm Depth : 1.6mm

Table 3.4 TIG-FSWelding condition

Welding condition		Values
TIG	Current(A)	60 ~ 80
	Shielding gas( L/min)	Ar 7 ~ 10
	CTWD(mm)	s = 5
	Torch angle	60°
FSW	Rotation speed(RPM)	300 ~ 700
	Welding speed(mm/s)	0.4 ~ 1.2
	Shoulder dia.(mm)	Ø18
	Pin dia.(mm)	Ø6.5
	Room temperature	20°
	Tilt angle	2 ~ 3°
TIG-FSW Distance = 16 ~ 20mm		
Leading condition = TIG leading		
Dia. of electrode = 2.4mm		



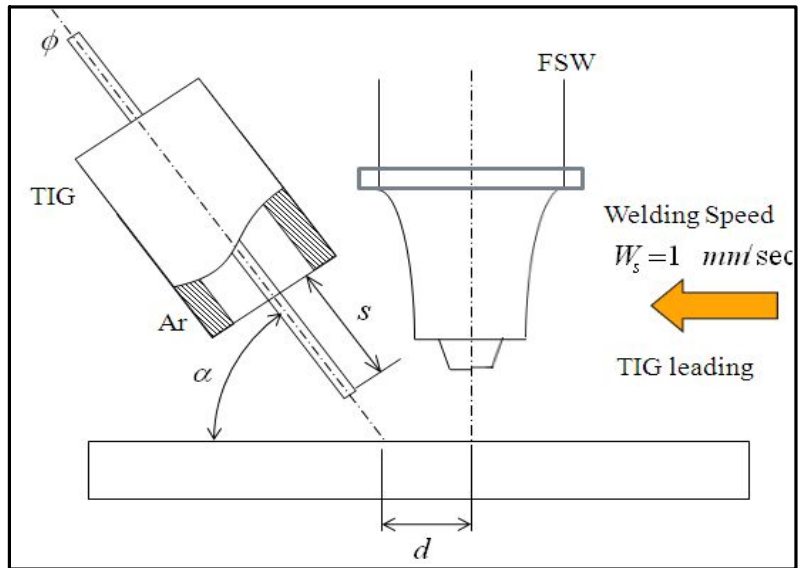


Fig. 3.6 Schematic of TIG assisted FSW welding process

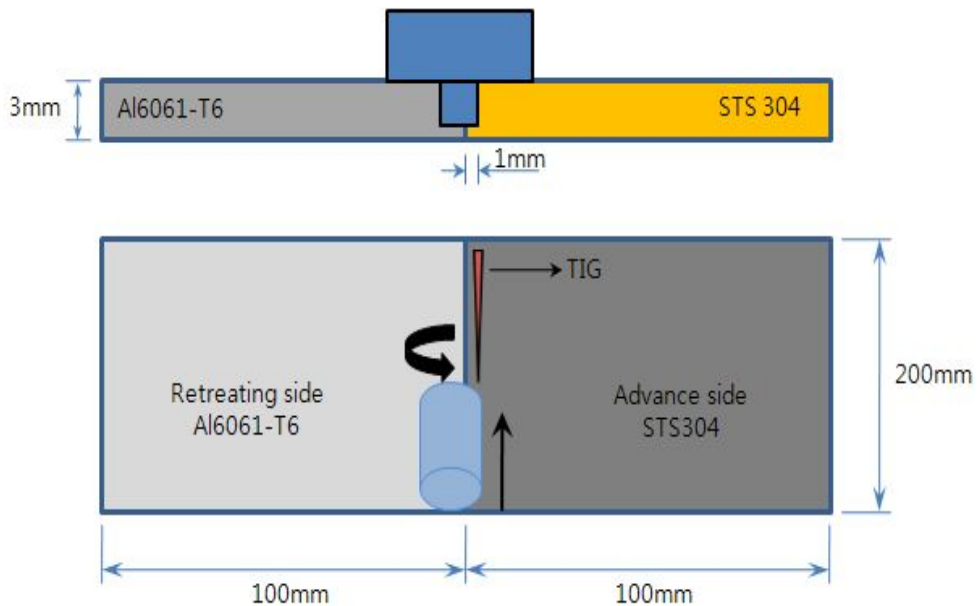


Fig. 3.7 Welding configuration for TIG-FSW

## 3.4 Experiment method

### 3.4.1 Tensile test

Tensile test was carried out with Dongil-Simaz Universal Testing Machine (EHF-EG200KN-40L) using WINSERVO program.

The specimens are fabricated in accordance with the national standards (KS0801-13-B). Tensile test was done with Load speed 0.05mm/sec Stress-Strain curve was obtained.

Fig. 3.8 shows the tensile testing setup and dimensions of the test specimen.

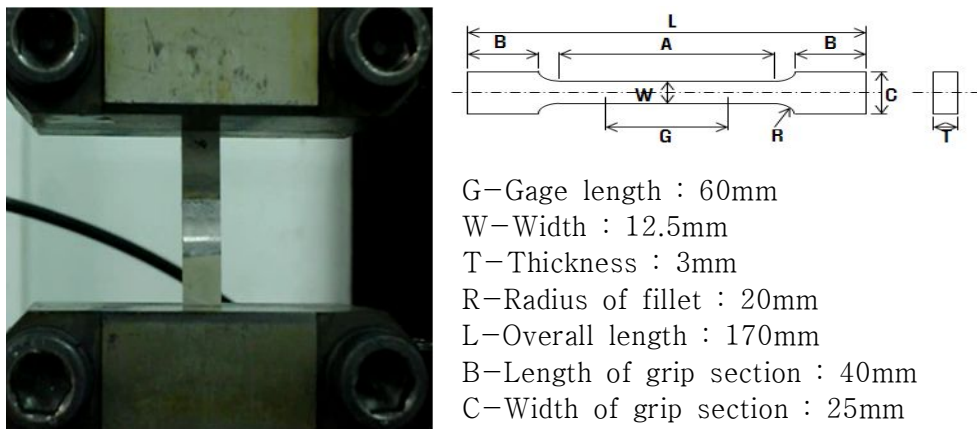


Fig. 3.8 Tensile test specimen dimensions

### 3.4.2 Hardness test

The hardness of a weld specimen was measured using Akashi HM-112 Vickers Hardness tester. The indenter employed in the Vickers test was a square-based pyramid whose opposite sides meet at the apex at an angle of  $136^\circ$  with load 500g applied for 10 sec.

Fig. 3.9 shows the Vickers hardness tester and test specimen. The hardness test was carried out on the welded specimen at 0.5gap at three different positions at 1mm distance apart.



Fig. 3.9 Vickers hardness test machine and specimen

### 3.4.3 Bending test

Guided bend tests are used to evaluate the ductility and soundness of welded joints and to detect incomplete fusion, cracking, delamination, effect of bead configuration, and macro-defects of welded joints. The quality of welds can be evaluated as a function of ductility to resist cracking during bending. Test beam with roller diameter  $\varnothing 20\text{mm}$  was loaded at mid-span of the weld specimen with bottom support at 50mm distance apart at a loading speed 30mm/min.

The bend test was carried out as per KS B 0803 standard.

Fig. 3.10 shows the bend test fixture and test specimen details.

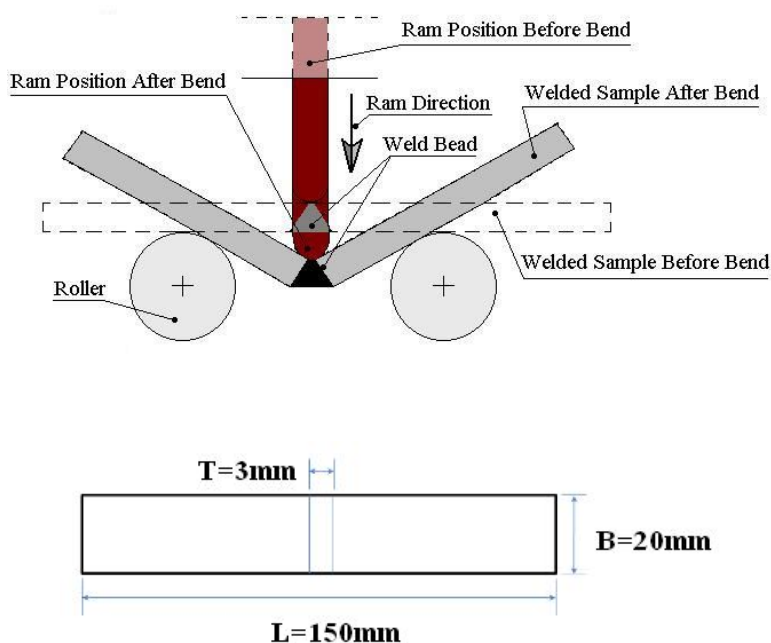


Fig. 3.10 Schematic of bending test fixture and bending test specimen dimension

### 3.4.4 Micro structure analyses

The cross section TIG assisted FSW specimen was cut and polished to observe the micro structure of the dissimilar joint. Proper etching of Al6061-T6 was done using the mixture of 1.5ml Nitric acid, 3ml Hydro chloric acid, 3ml Hydro fluoric acid and 100ml distilled water. STS304 was properly etched using 10% oxalic acid and 90% distilled water.

The prepared specimen was mounted on OLYMPUS optical microscope to observe the micro structure as shown in Fig. 3.11.



Fig. 3.11 Optical microscope

# Chapter 4

## EXPERIMENTAL INVESTIGATION & RESULTS

### 4.1 Welding condition and bead shape

#### 4.1.1 Experiment by TIG welding

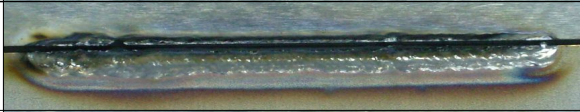
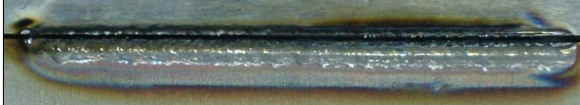
Table 4.1(a) shows the TIG welding parameters used for this experiments. The material properties of Al6061-T6 and STS304 are different and the melting point of STS304 is two times higher than Al6061-T6 and therefore during welding, melting of Al6061-T6 occurs prior to STS304. Thus it was considered that it makes impossible to join dissimilar weld with TIG welding process. The bead shapes obtained for dissimilar weld with TIG is given in Table 4.1(b).

**Table 4.1 TIG welding parameters and obtained bead shapes**

#### (a) Welding parameters

No.	Material	Plunge point	Travel speed (mm/s)	TIG Current (A)	TIG pulsed Current (A)	Shield Gas ( l/min)	Torch Angle (deg)
1	Al-STs	center	1.0	120	100	7	60
2	Al-STs	center	1.0	120	80	7	60

#### (b) Weld bead of dissimilar joint

TIG Current(A)	Travel speed (mm/s)	Bead appearance
120	1.0	
100	1.0	

#### 4.1.2 Experiment by Friction stir welding

From many trials of experiment carried out on dissimilar joint by FSW, best 15 number of trials was taken in to account and is tabulated as given in Table 4.2(a). The bead shapes of the best 15 trials are shown in table 4.2(b). Rotation speed of the tool, tool travel speed and tool rotating direction were varied to obtain better results. Initial trials were done for obtaining better surface beads with proper exit holes. Over 700RPM and 1mm/sec, from the macro images, it was observed that the presence of stainless steel deposits are more in the aluminium stir zone which can seriously affect the mechanical characteristics of weld joint. From the FSW experiments and macro images, tool rotation at 400 and 500RPM at tool travel speed 0.6~0.8mm/s was found good and considered to carry out TIG assisted FSW experiments. Between 600~ 700RPM more heat was generated due to friction at the tool-workpiece interface and thus higher amount of STS304 inclusions were found in the Al6061-T6 stir zone.















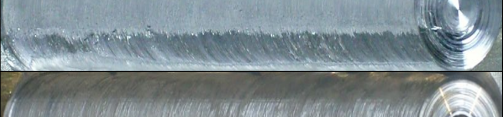






**Table 4.2 FSW parameters and obtained bead shapes**

**(a) Welding parameters**

No.	Material	Adv. side	Tool plunge point	Rotating Speed (rpm)	Travel Speed (mm/s)	Rotation Direction
1	Al–STS	STS	9:1	400	0.8	cw
2	Al–STS	STS	9:1	400	0.8	ccw
3	Al–STS	STS	9:1	400	0.6	cw
4	Al–STS	STS	9:1	400	0.6	ccw
5	Al–STS	STS	9:1	500	0.6	cw
6	Al–STS	STS	9:1	500	0.6	ccw
7	Al–STS	STS	9:1	600	0.6	cw
8	Al–STS	STS	9:1	600	0.6	ccw
9	Al–STS	STS	9:1	700	0.6	cw
10	Al–STS	STS	9:1	700	0.6	ccw
11	Al–STS	STS	9:1	700	0.8	cw
12	Al–STS	STS	9:1	700	0.8	ccw
13	Al–STS	STS	9:1	500	1.0	ccw
14	Al–STS	STS	9:1	600	1.0	ccw
15	Al–STS	STS	9:1	700	1.0	ccw



(b) Weld beads and macro images of dissimilar joint

RPM	Travel speed	Bead appearance	Macro image
400	0.6		
	0.8		
500	0.6		
	0.8		
	1.0		
600	0.6		
	0.8		
	1.0		
700	0.6		
	0.8		
	1.0		—

### 4.1.3 Experiment by TIG Assisted Friction stir welding

Table 4.3 (a) and (b) shows the TIG assisted FSW parameters and obtained bead shapes for dissimilar joint of Al6061-T6 and STS304 butt joint. For TIG-FSW process, the best welding parameters obtained from the FSW experiments and TIG preheating BOP test conditions were considered respectively. 41 trials was carried out by varying different welding parameters to achieve the optimum welding condition. At, tool rotation speed between 300~400RPM, TIG current of 70(A) and shield gas flow rate of 7 L/min, excellent bead shape was obtained and no weld defects was found in the cross sectional macro image. Above 500RPM tool rotation speed with TIG preheating, more heat was generated due to friction at the tool-workpiece interface and thus higher amount of STS304 inclusions were found in the Al6061-T6 stir zone.

**Table 4.3 TIG Assisted FSW parameters and obtained bead shapes**

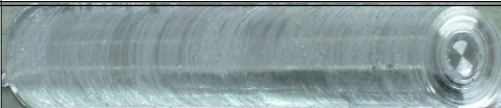
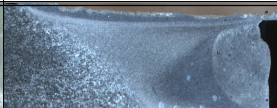



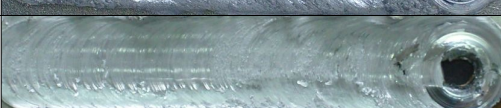

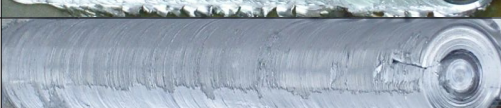









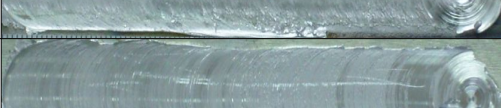

**(a) Welding parameters**

No.	Material	Tool plunge point	Rotati ng Speed	Travel Speed	Rotati on Direct ion	TIG Curre nt(A)	TIG pulsed Curre nt(A)	Shield Gas( L /min)	Torch Angle
1	Al–STS	9:1	300	0.6	ccw	80	80	7	60
2	Al–STS	9:1	300	0.8	ccw	80	80	7	60
3	Al–STS	9:1	300	1.0	ccw	0	80	7	60
4	Al–STS	9:1	400	0.2	ccw	60	60	7	60
5	Al–STS	9:1	400	0.4	ccw	60	60	7	60
6	Al–STS	9:1	400	0.6	ccw	60	60	10	60
7	Al–STS	9:1	400	0.8	ccw	60	60	10	60
8	Al–STS	9:1	400	1.0	ccw	60	60	10	60
9	Al–STS	9:1	400	1.0	ccw	80	80	7	60
10	Al–STS	9:1	400	1.2	ccw	100	100	10	60
11	Al–STS	9:1	400	1.4	ccw	100	100	10	60













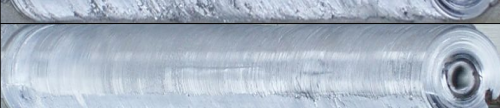



No.	Material	Tool plunge point	Rotati ng Speed	Travel Speed	Rotati on Direct ion	TIG Curre nt(A)	TIG pulsed Curre nt(A)	Shield Gas( L /min)	Torch Angle
12	Al-STS	9:1	500	1.0	ccw	70	30	20	60
13	Al-STS	9:1	500	1.0	ccw	80	30	20	60
14	Al-STS	9:1	400	1.0	ccw	85	30	20	60
15	Al-STS	9:1	400	1.0	ccw	85	30	20	60
16	Al-STS	9:1	500	0.9	ccw	60	60	20	60
17	Al-STS	9:1	500	1.0	ccw	60	60	20	60
18	Al-STS	9:1	500	1.0	ccw	70	70	20	60
19	Al-STS	9:1	500	1.0	ccw	80	80	20	60
20	Al-STS	9:1	500	0.8	ccw	60	60	15	60
21	Al-STS	9:1	500	0.8	ccw	60	60	10	60
22	Al-STS	9:1	500	0.8	ccw	70	70	10	60
23	Al-STS	9:1	500	0.8	ccw	80	80	10	60
24	Al-STS	9:1	500	0.6	ccw	60	60	10	60
25	Al-STS	9:1	500	0.6	ccw	70	70	10	60
26	Al-STS	9:1	500	0.6	ccw	80	80	10	60

No.	Material	Tool plunge point	Rotati ng Speed	Travel Speed	Rotati on Direct ion	TIG Curre nt(A)	TIG pulsed Curre nt(A)	Shield Gas( L /min)	Torch Angle
27	Al-STs	9:1	400	0.6	ccw	60	60	10	60
28	Al-STs	9:1	400	0.8	ccw	60	60	10	60
29	Al-STs	9:1	400	1.0	ccw	60	60	10	60
30	Al-STs	9:1	600	0.6	ccw	60	60	10	60
31	Al-STs	9:1	600	0.8	ccw	60	60	10	60
32	Al-STs	9:1	600	1.0	ccw	60	60	10	60
33	Al-STs	9:1	600	1.2	ccw	70	70	10	60
34	Al-STs	9:1	600	1.0	ccw	70	70	10	60
35	Al-STs	9:1	600	0.8	ccw	70	70	7	60
36	Al-STs	9:1	600	0.6	ccw	70	70	7	60
37	Al-STs	9:1	600	0.4	ccw	60	60	7	60
38	Al-STs	9:1	400	0.4	ccw	60	60	7	60
39	Al-STs	9:1	500	0.4	ccw	60	60	7	60
40	Al-STs	9:1	700	0.8	ccw	70	70	7	60
41	Al-STs	9:1	700	1.0	ccw	70	70	7	60

(b) Weld beads and macro images of dissimilar joint

RPM	Travel speed	Appearance	Macro image
300	0.6		
	0.8		
	1.0		—
400	0.2		
	0.4		
	0.6		
	0.8		
	1.0		
	1.2		
	1.4		




RPM	Travel speed	Bead appearance	Macro image
500	0.6		
	0.8		
	1.0		
600	0.6		
	0.8		
	1.0		
700	0.8		
	1.0		

## 4.2 Tensile test results

### 4.2.1 Tensile test of similar joint (Al6061-T6)

Tensile test of similar joint of Al6061-T6 was carried out to understand the tensile strength of FSW joint made at 400RPM and 1mm/sec tool travel speed (Table 4.4). Testing was carried out as per korean standards. This result was used as a reference for the testing of TIG-FSW dissimilar joint. The tensile test results were shown in Fig4.1. The tensile strength of the FSW weld joint was obtained as 245MPa which is 80% of the tensile strength of base metal (310MPa).

Table 4.4 Bead appearance of similar joint specimen considered for tensile test

RPM	Travel speed(mm/s)	Appearance
400	1	

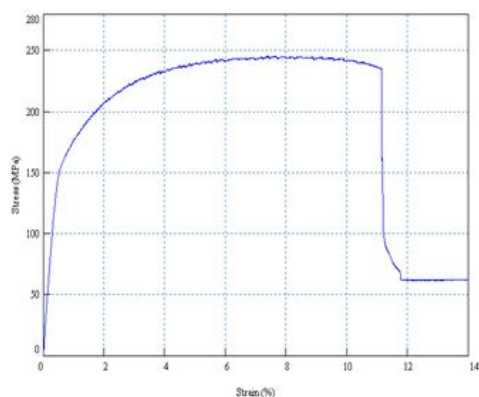


Fig. 4.1 Tested specimen and Stress-Strain curve



#### 4.2.2 Tensile test of FSW dissimilar joint

Testing of tensile strength of dissimilar weld joint by FSW was carried out as per korean standards. The tensile test results (Table 4.5) reveals that fracture occurs at the dissimilar joining interface. The fracture was occurred at the Al6061-T6 stir zone where STS304 inclusions are more.

From stress-strain curve it is evident that the specimen is subjected to brittle fracture (Table 4.6). Good tensile strength is obtained for the weld joint made at tool rotation 500RPM and travel speed 0.6mm/s.

Table 4.5 Cross sections and fractured specimens of dissimilar joint by FSW










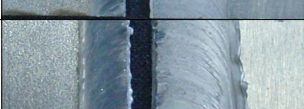











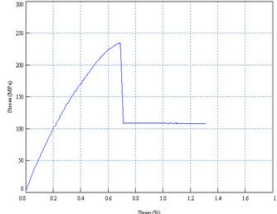
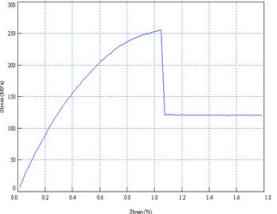
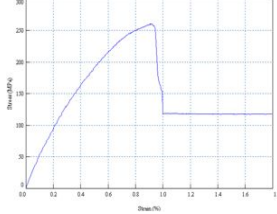
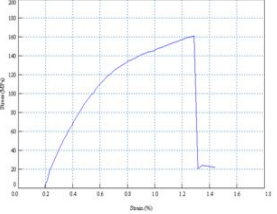
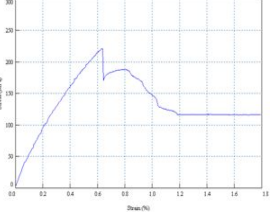
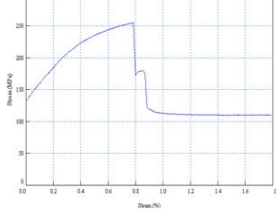
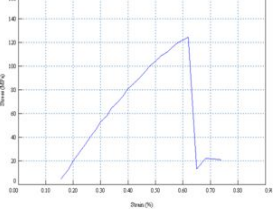
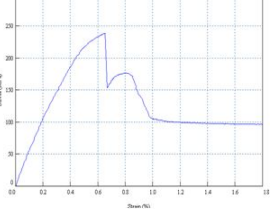
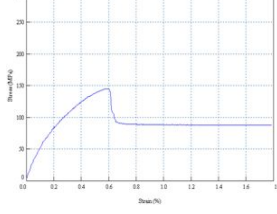
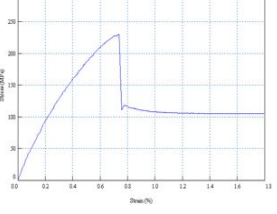
RPM	Travel speed	Macro image	Fractured specimens	T.S(MPa)
400	0.6			234
	0.8			255
500	0.6			260
	0.8			160
	1.0			220
600	0.6			255
	0.8			124
	1.0			238
700	0.6			144
	0.8			230
	1.0	—		교반불량






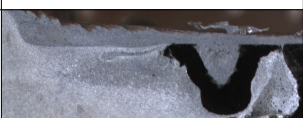
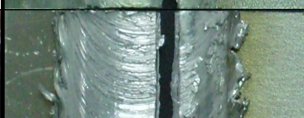












Table 4.6 Stress–strain curve for dissimilar weld joint by FSW

RPM	Travel speed(mm/s)		
	0.6	0.8	1.0
400			—
500			
600			
700			—

### 4.2.3 Tensile test of TIG assisted FSW dissimilar joint

Table 4.7 shows the cross sections and fractured specimens of dissimilar joint by TIG assisted FSW. As observed from the tensile test results, the fracture occurred at the joining interface in specimens welded at 300 and 400RPM tool rotation speed. Above 400RPM the fracture occurred little across the Al6061-T6 weld nugget. The tensile strength of dissimilar joint by TIG-FSW was found 80~90% than that of Al6061-T6 base metal. The good tensile strength obtained was 290MPa (Al6061-T6 base metal tensile strength 310MPa) i.e, about 93% than that of base metal at tool rotation speed 300RPM, travel speed 0.8mm/s and TIG current 70A. The stress-strain curve (Table 4.8) shows that the specimen is fractured in a brittle manner with little plastic deformation.

Table 4.7 Cross sections and fractured specimens of dissimilar joint by TIG assisted FSW

RPM	Travel speed	Macro	Fractured specimens	T.S(MPa)
300	0.6			269
	0.8			290
	1.0	—		261
400	0.2			172
	0.4			226
	0.6			233
	0.8			258
	1.0			268
	1.2			267
	1.4			262



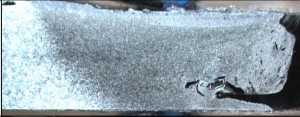

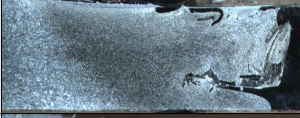
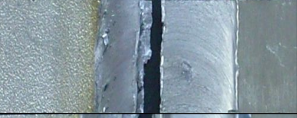











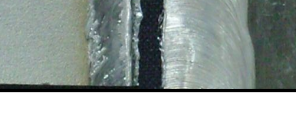
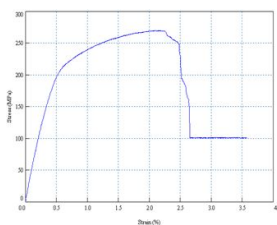
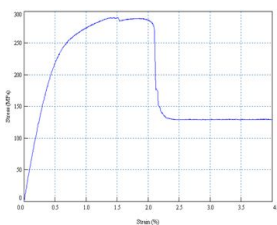
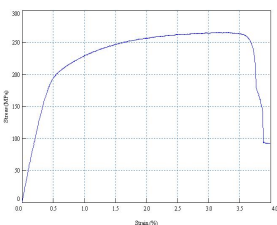
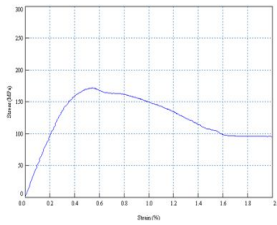
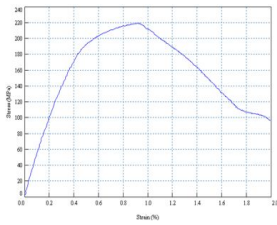
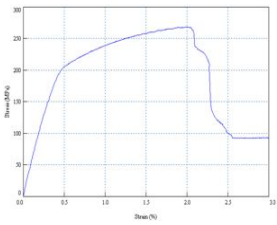
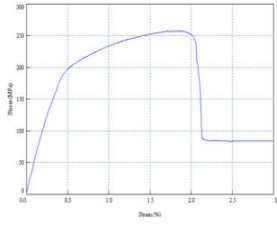
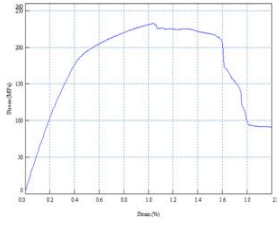
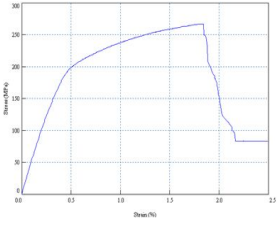
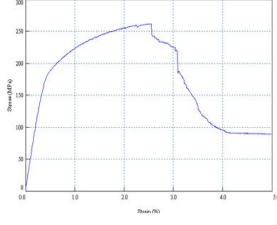
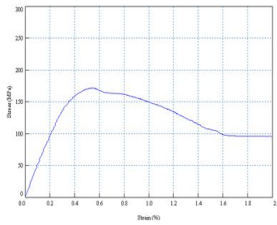
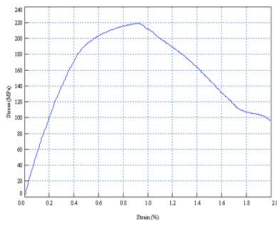
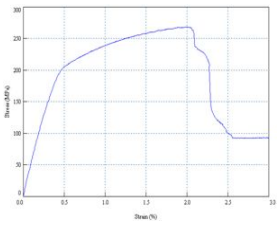
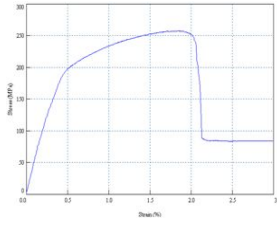
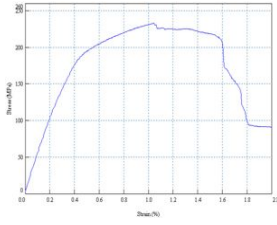
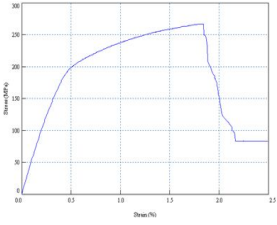
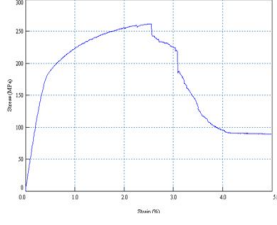
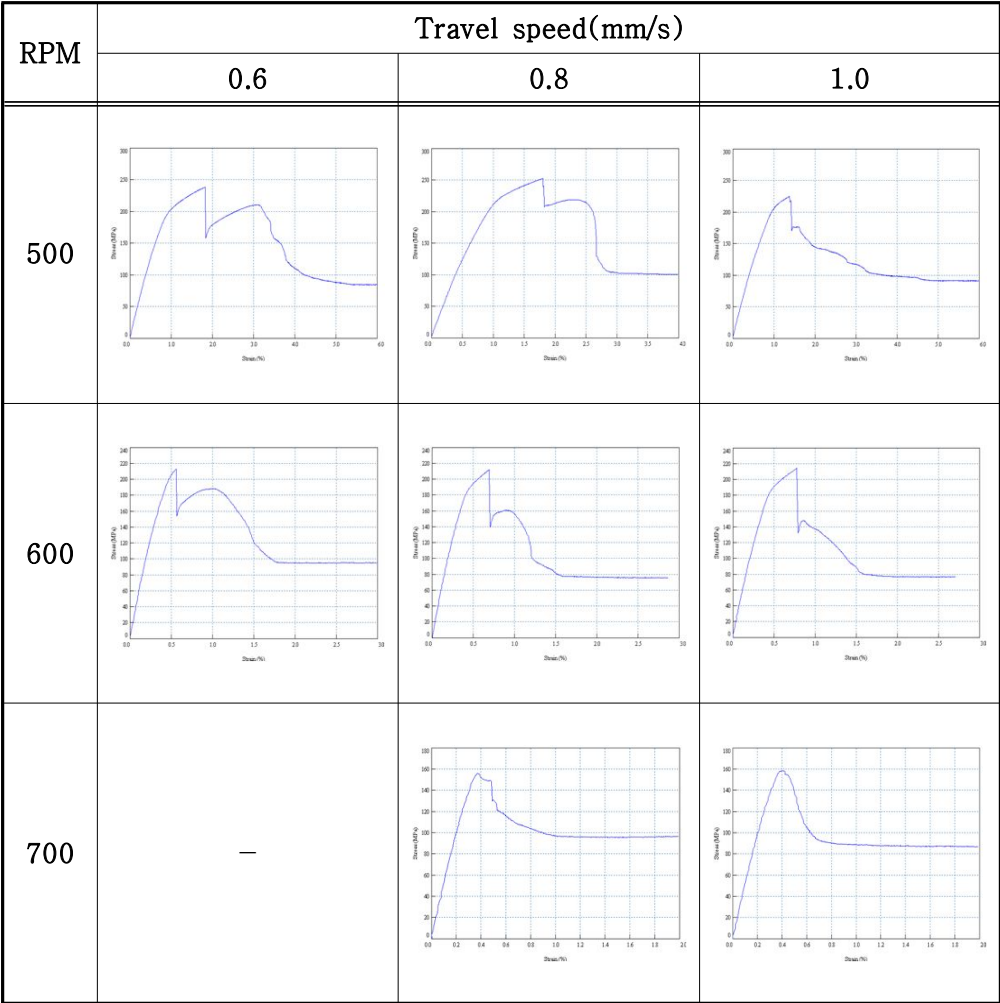
RPM	Travel speed	Macro image	Fractured specimens	T.S(MPa)
500	0.6			216
	0.8			252
	1.0			224
600	0.6			201
	0.8			214
	1.0			214
700	0.8			156
	1.0			158

Table 4.8 Stress–strain curve for dissimilar weld joint by  
TIG assisted FSW

RPM	Travel speed(mm/s)		
	0.6	0.8	1.0
300			
	0.2	0.4	0.6
			
	0.8	1.0	1.2
			
	1.4	—	—
		—	—
400	0.2	0.4	0.6
			
	0.8	1.0	1.2
			
	1.4	—	—
		—	—





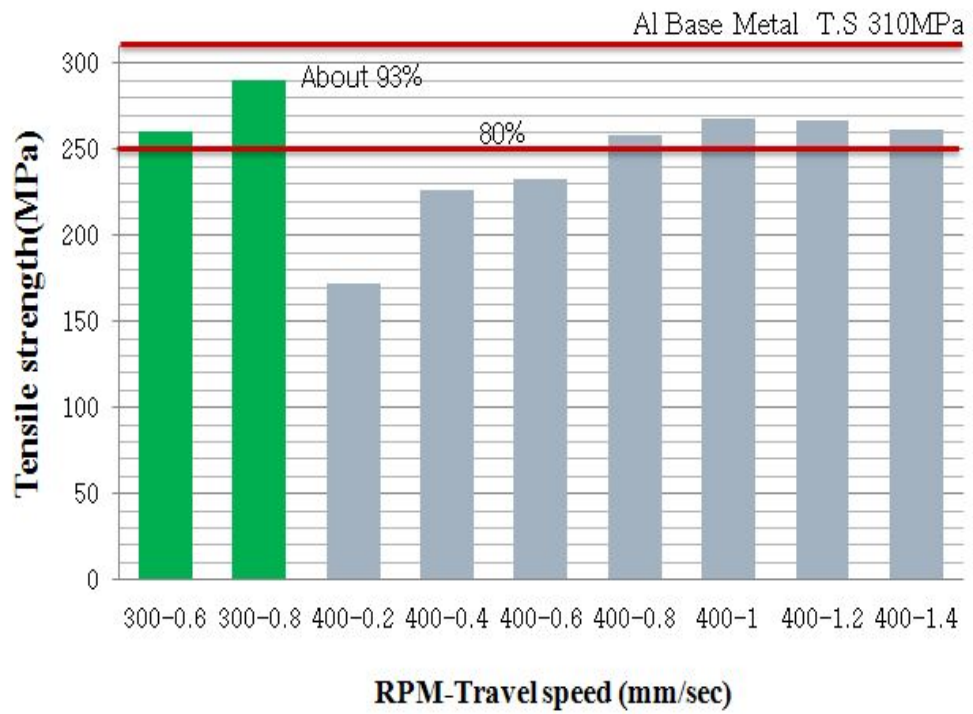


Fig. 4.2 Tensile test result of welded specimen

### 4.3 Hardness test results

The hardness distributions of dissimilar joint by TIG-FSW is shown in Fig.4.3. The hardness at the TMAZ and HAZ is approximately 50% of the base metal before welding and is a characteristic of dynamic recrystallization that appears to provide a mechanism for solid state welding. The hardness values near the top of the weld are approximately between 54 and 57 Hv in contrast to 56 to 59 Hv near the bottom of the weld as shown in Fig. 4.5. Though frictional heating is greater near the top surface where maximum temperatures occurs, there is no much difference in hardness values at top and bottom of the stir zone. The difference in values at base metal, TMAZ and HAZ indicates that softening of material occurred due to plastic flow.

The hardness value at the weld bond line side sharply decreased towards the weld nugget from the level of the thermo-mechanically affected zone in the stainless steel at advancing side of weld. The hardness of the weld nugget shows variable values because of the presence of the fine or coarse dispersed stainless steel particles in the weld nugget.

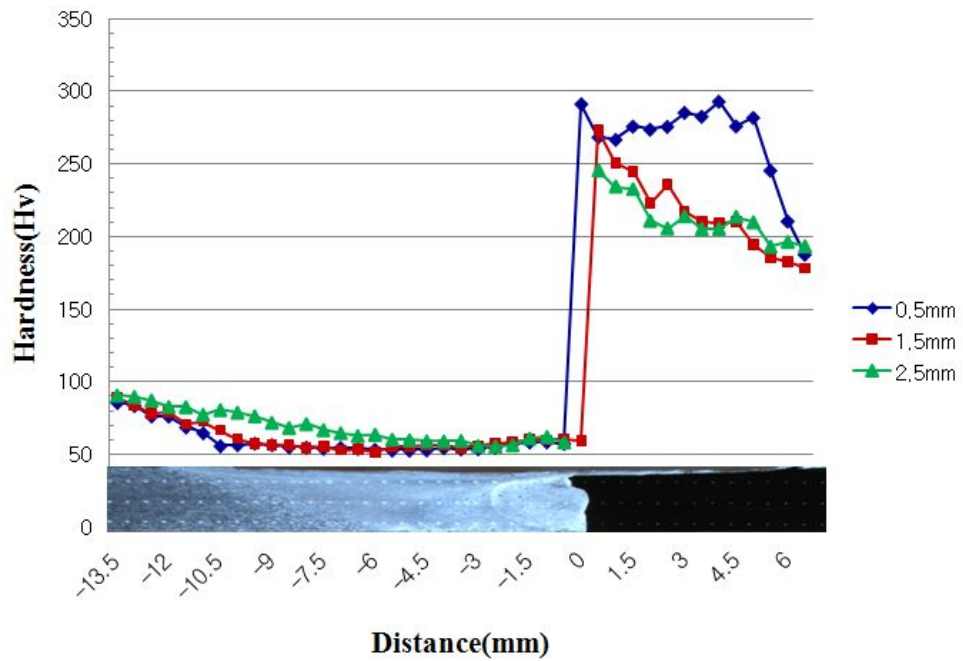


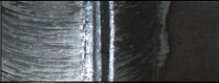
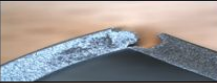





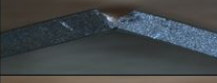



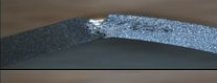




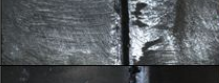





Fig. 4.3 Hardness distribution of dissimilar(TIG assisted FSW)

## 4.4 Bending test results

It is a known fact that mechanical properties of Al6061-T6 and STS304 are different, so there is no meaning in conducting mechanical bend test for dissimilar joint weld by TIG-FSW. But to take it as reference for future research work, three point bending test has been done for the dissimilar weld specimen. Fracture occurred in all welded specimens at joining interface and weld nugget zone during surface and root bend test.

Table 4.9 shows the bending test results of dissimilar joint by TIG-FSW.

Table 4.9 Bending test results

RPM	Travel speed	Bend position	Surface Fracture	Lateral Fracture	Load (kgf)	Displacement (mm)	Fracture position
300	0.6	Face bend			56.2	12.5	Bond line
		Root bend			56.2	9.8	Nugget zone
	0.8	Face bend			51	4.3	Bond line
		Root bend			35.7	8	Bond line
	1.0	Face bend			56.2	7.6	Bond line
		Root bend			56.2	13	Bond line
400	0.6	Face bend			45.9	7.4	Bond line
		Root bend			56.2	40	Good
	0.8	Face bend			56.2	11	Bond line
		Root bend			61.4	16.6	Nugget zone
	1.0	Face bend			56.2	40	Good

## 4.5 Microstructure analyses of dissimilar joint

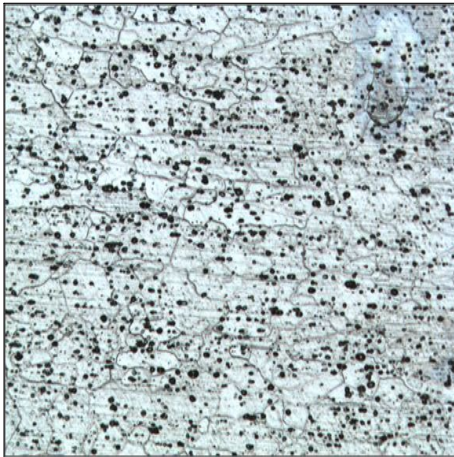
### 4.5.1 Microstructure of FSW dissimilar joint

Microstructure of FSW dissimilar joint is shown in Fig. 4.4. The base Al6061–T6 alloy contains elongated grains in the rolling direction. The Al6061–T6 alloy in the weld nugget consists of fine, equiaxed, recrystallized grains. The fine recrystallized grains in the stirred zone are attributed to the generation of high deformation and temperature during FSW.

The weld nugget exhibits a mixture of Al6061–T6 alloy and STS304 particles pulled away by force of tool pin from the STS304 surface. Therefore the weld nugget has a composite structure of STS304 particles reinforced Al6061–T6 alloy. STS304 particles inclusions were more in the Al6061–T6 weld nugget and have an irregular shape and inhomogeneous distribution within the weld nugget.

### 4.5.2 Microstructure of TIG assisted FSW dissimilar joint

Microstructure of FSW dissimilar joint is shown in Fig. 4.5. From the microstructure image of Al6061–T6 base metal, it is clear that the base metal have the same microstructure with homogeneous grain distribution as in FSW. Compared to FSW process, only finer particles of STS304 inclusions were found in TIG–FSW microstructure. The structure of base stainless steel shows typically coarse austenitic grains. Due to preheating effect at STS304 plate the grain size is increased at HAZ.



(A) Al-B.M



(B) HAZ, TMAZ



(C) Weld nugget zone

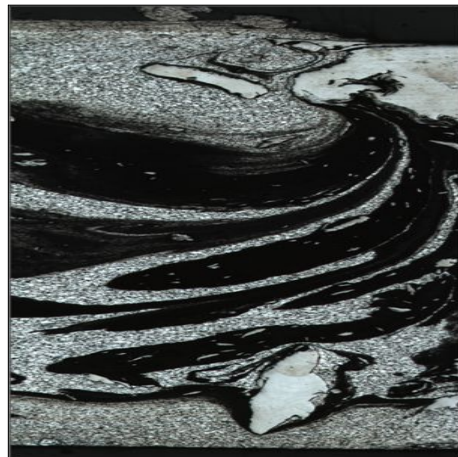
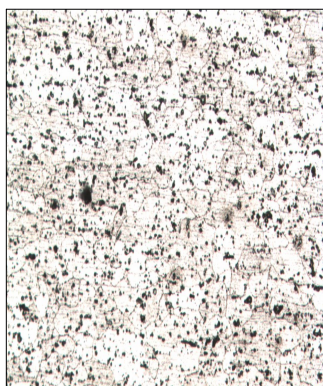
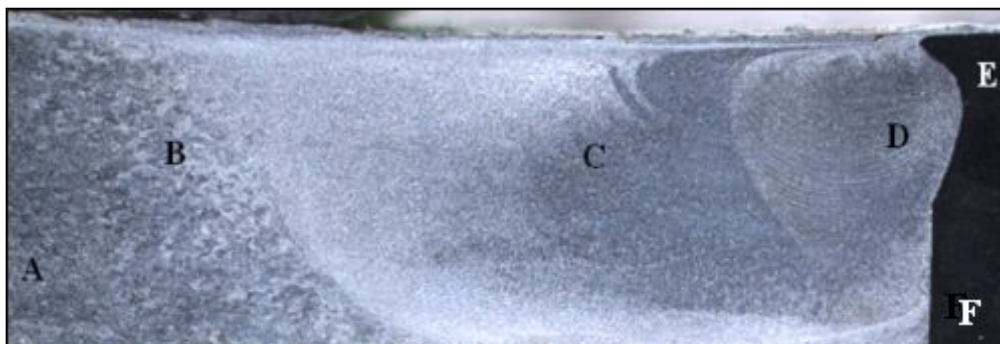


Fig. 4.4 Microstructural(FSW)

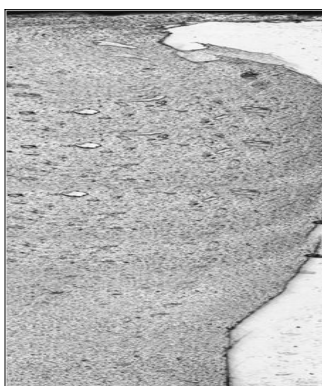




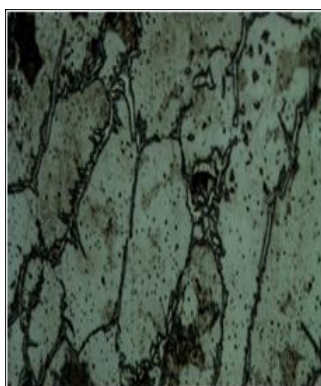
(A) Al-B.M



(B) HAZ, TMAZ



(D) Weld nugget zone



(E) STS-HAZ



(F) STS-B.M

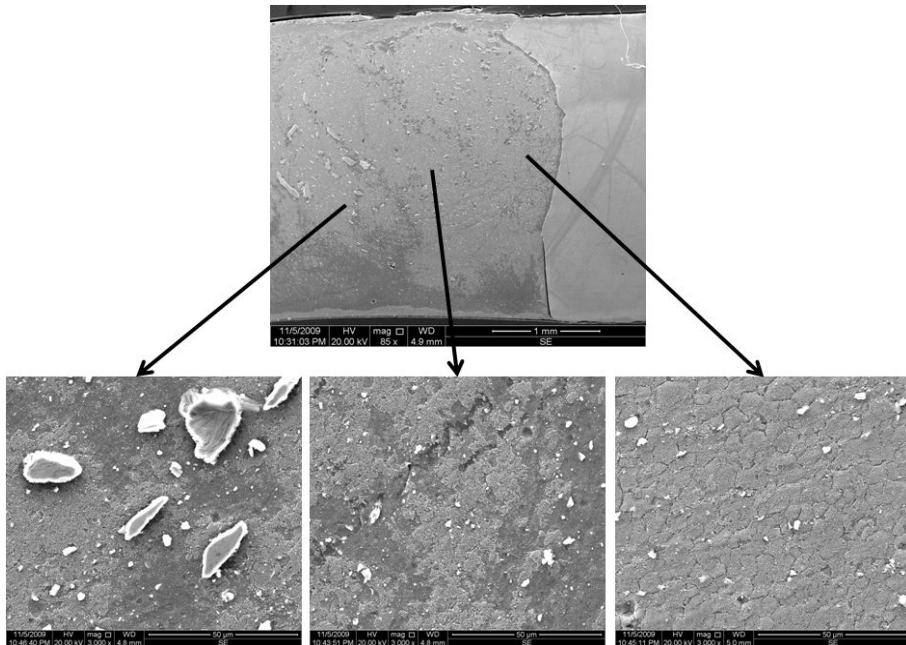
Fig. 4.5 Microstructural(TIG assisted FSW joint)



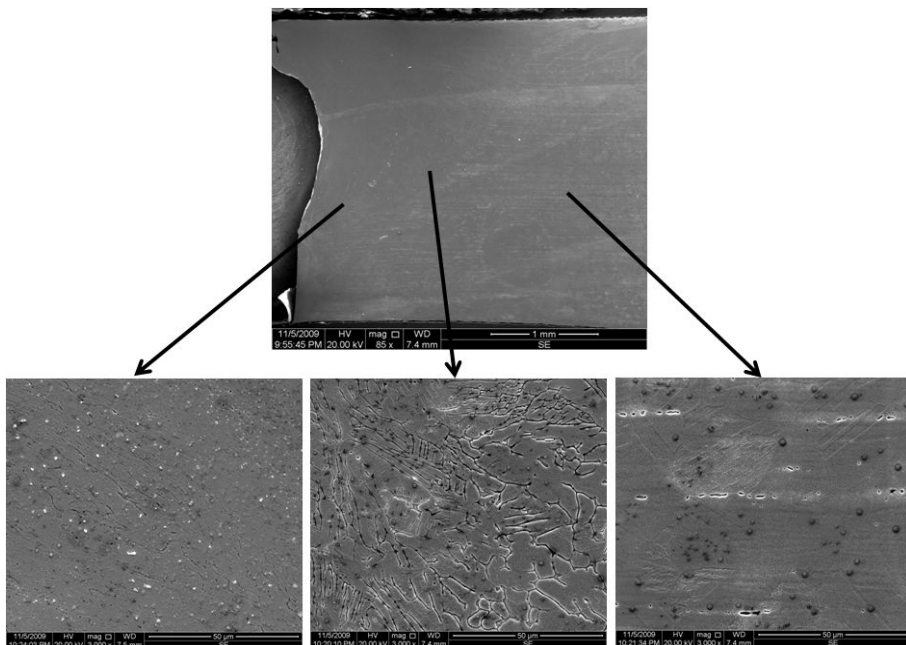
### 4.5.3 Microstructure analyses by using SEM and EDS

The weld nugget exhibits a mixture of Al 6061-T6 alloy and STS304 particles pulled away by force of tool pin from the STS304 surface. Therefore the weld nugget has a composite structure of STS304 particles reinforced Al 6061-T6 alloy. Fig. 4.6 (a) and (b) Fig. 2 shows SEM of the cross section of the TIG assisted friction stir welded dissimilar Al6061-T6 alloy to STS304. STS304 particles on Al 6061-T6 alloy were found in the weld nugget. (b) shows the STS304 microstructure of weld joint. However, re-crystallization of Al6061-T6 might have occurred in the weld zone with grain size very much smaller than STS304. From Fig. 4.7 (a) and (b), it is found that the ductile fracture occurred at weld nugget towards Al6061-T6 direction. The tool pin height is limited by work piece thickness and will not penetrate the workpiece. Therefore the crack is found originated at a depth where the tool pin interacts with the workpiece. Ductile fracture with dimple pattern is observed on the specimen fracture surface, when fractured with tensile load applied at transverse direction. At cleavage face of the grain boundary the brittle fracture is found at area where plastic deformation has not occurred.

From the EDS image of weld nugget zone along Al6061-T6 side, Fig. 4.8(a), at point 1, the chemical compound of Al6061-T6 is same as that of base metal, at point 2 fewer amount of Cr and Fe from STS304 is found and at point 3 chemical compounds of STS304 is found more with little Al6061-T6 compounds. Along STS304 side, Fig 4.8(b), only STS304 chemical compounds were found at point 1 and 2. The region where the diffusion of the Al6061-T6 does not reached can be judged from the image.

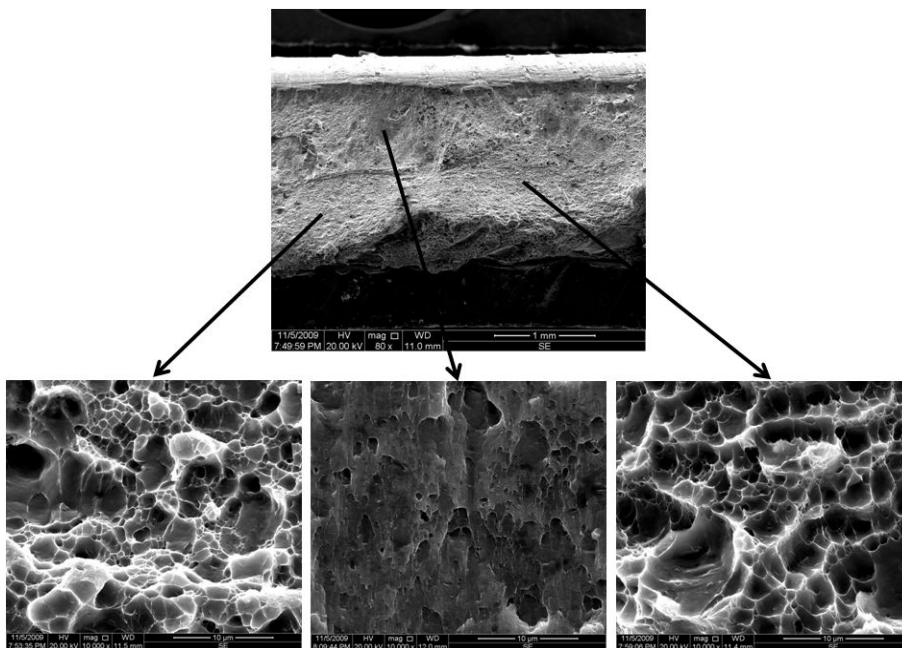


(a) Direction of Al6061-T6

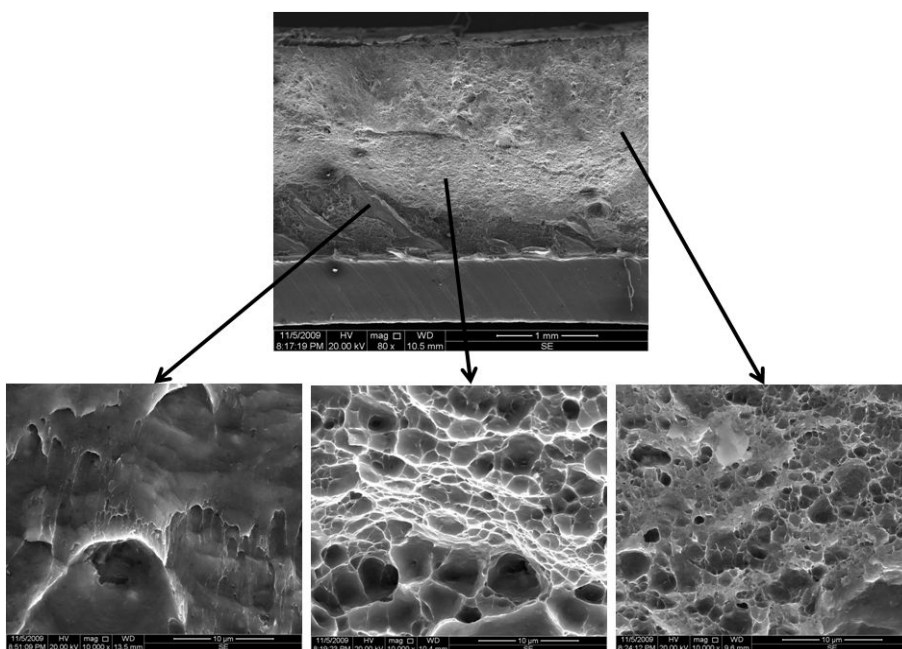


(b) Direction of STS304

Fig. 4.6 SEM micrograph of dissimilar weld

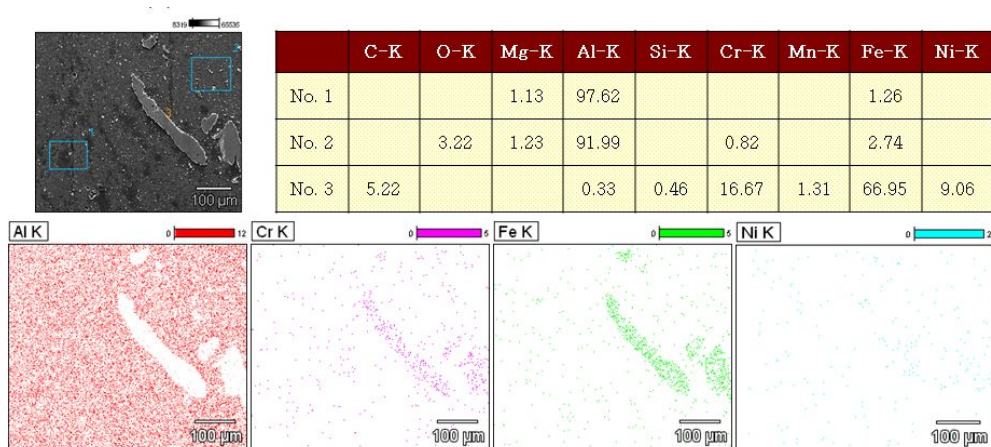


(a) Direction of Al6061-T6

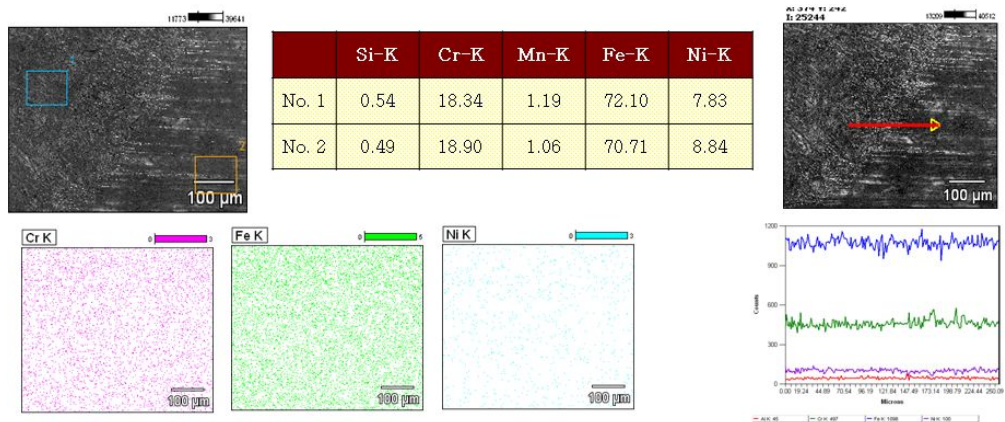


(b) Direction of STS304

Fig. 4.7 SEM of dissimilar weld tensile fracture surface



(a) Chemical compounds of Al6061–T6 weld



(b) Chemical compounds of STS304 weld

Fig. 4.9 EDS analysis of dissimilar weld

## Chapter 5

### CONCLUSION

A new welding technique, TIG-FSW, was successfully applied to the joining of Al6061-T6 STS304. The microstructure, hardness, tensile strength and bending of friction stir welded dissimilar Al6061-T6 alloy and STS304 joints have been studied in the present work.

1. To achieve a good weld joint between Al6061-T6 and STS304, the tool plunge position was adjusted towards Al6061-T6 side to soften Al material and tool was made to rotate in counter clock wise direction. Al6061-T6 was placed in the retreating side and STS304 in the advancing side for conducting this welding experiment process. This is because the soften material flows in the direction of tool rotation and therefore the soften Al material flow was found to be good when Al was placed in the retreating side.
2. The tensile strength was found not satisfactory when the rotating speed was above 600RPM. Also, irregular shape and inhomogeneous distribution of STS304 inclusions were found in the Al6061-T6 weld nugget.
3. In FSW of dissimilar joint, because of the maximum plunge force area, the heat generation was maximum at Al6061-T6 side which lead to brittle fracture of the weld joint. Hence, TIG-FSW process helps to balance the heat generation at both Al6061-T6 and STS304 which increased the tensile strength of the dissimilar weld join. The tensile strength of dissimilar joint by FSW was found 60~80% that of Al6061-T6 base metal where as tensile strength was 80~90% when joined with TIG-FSW.
4. The best welding joint was obtained at tool rotation speed 300RPM, travel speed 0.8mm/s and TIG current 70A. The tensile strength was obtained as 290MPa (Al6061-T6 base metal tensile strength 310MPa

- ) i.e, about 93% than that of base metal. The best conditions was obtained between tool rotation speed 300~400RPM and travel speed 0.6~1.4mm/s and the tensile strength was about 80% than that of base metal.
5. The hardness values were found different in the weld nugget of dissimilar joint depending upon the material properties. The hardness value at the retreating side sharply decreased towards the weld nugget from the level of TMAZ in the stainless steel at advancing side of weld. The hardness at the weld nugget across Al6061-T6 bond line are not seriously affected by presence of STS304 deposits.
  6. SEM of the cross section of the TIG assisted friction stir welded dissimilar Al6061-T6 alloy to STS304. Stainless steel particles on Al 6061-T6 alloy were found in the weld nugget. STS304 micro structure of weld joint. However, re-crystallization of Al6061-T6 might have occurred in the weld zone with grain size very much smaller than STS304.

Finally, it is concluded that TIG assisted FSW process can be applied to dissimilar Al6061-T6 and STS304 successively in industrial applications.

## REFERENCES

- [1] H.S. Bang, H.S. Bang, S.M. Joo, "Numerical simulation of Al-SPCC weldment", Key Engineering Materials, P1738~1744, Oct., 2006
- [2] Y.J.Chao, and X.Qi: Heat transfer and thermo-mechanical analysis of Friction Stir joining of Al6061-T6 plates, 1st International Symposium on Friction Stir Welding, (1999).
- [3] A.Askari, S.Silling, B.London, and M.Mahoney: Modelling and Analysis of Friction Stir Welding Processes, Friction stir welding and Processing, TMS publication,(2001) p.43.
- [4] A.William, Using Gleeble flow stress data to establish optimum FSW processing parameter in Aluminium Alloys, Advanced material processing centre, (2002).
- [5] H.S. Bang. "Study on The Mechanical Behaviour of Welded part in thick Plate - Three-dimensional Thermal Elasto-Plastic Analysis Baseon Finite Element Method." Journal of the Korean Welding Society, Vol.10, No.4, pp.37~43, December 1992.
- [6] Rajesh S.R., "Development of mathematical model for Thermo - mechanical behavior of Friction Stir Welding an introduction Soldering by using FEM/BEM", 2007
- [7] W.B. Lee, S.B. Jung, Gehard Biallas, Martin Schmuecker. "Joint properties and Interface Analysis of Friction Stir Welded Dissimilar Materials between Austenite Stainless Steel and 6013 Al Alloy" Journal of the Korean Welding Society, Vo.23, No.5, pp.469~476, October 2005.
- [8] H. Kokawa, S.H.C. Park, Y.S. Sato, K. Okamoto, S. Hirano, M. Inagaki : Microstructures in Friction Stir Welded 304 Austenitic Stainless Steel, Welding in the World, 49(3/4), 2005, pp.34-40
- [9] T.J. Lienert, W.L. Steelwag, Jr., B.B Grimmett, and R.W. Warke : Friction Stir Welding Studies on Mild Steel, Welding Journal, 82(1),

2003, pp.1S–9S

- [10] AWS, WELDING HANDBOOK, Vol.1, Eighth Edition, 1987.
- [11] AWS, WELDING HANDBOOK, Vol.2, Eighth Edition, 1991.
- [12] W.M. Thomas, P.L.Threadgill, and E.D. Nicholas : Feasible of Friction Stir Welding Steel, Science and Technology of Welding and Joining, 4(6), 1999, pp. 365–372
- [13] L.E.Murr, et al.: Solid–state flow association with the friction stir welding of dissimilar metals, Fluid flow phenomena in metals processing (1999), 31–40
- [14] Huseyin Uzun, Claudio Dalle Donne, Alberto Argagnotto, Tommaso Ghidini, Carla Gambaro.:Friction stir welding of dissimilar Al 6013–T4 To X5CrNi18–10 stainless steel, Materials and Design 26 (2005) 41–46
- [15] Z. Sun, R. Karppi, "The application of electron beam welding for the joining of dissimilar metals: an overview", Journal of materials processing technology 59 (1996) 257–267
- [16] H.S. Bang, G.Y. Han, "The plane–deformation thermal elasto–plastic analysis during welding of plate", The society of naval architects of korea p33~40, Apr.1994
- [17] S. Katayama, et al.: Proc.5th Int.Conf.on TRENDS IN WELDING RESEARCH, Georgia, June (1998), pp.467–472.
- [18] WELDING HANDBOOK, Eighth Edition, Volume 3, MATERIALS AND APPLICATION PART 1, pp.100~110, AMERICAN WELDING SOCIETY.
- [19] E. G. WEST, THE WELDING OF NON–FERROUS METALS, CHAPMAN & HALL LTD, 1951, pp.129~254.
- [20] Hidekazu Murakawa and Jianxun Zhang, "FEM Simulation of welding process (Report I)", Trans. JWRI, Vol. 27, No. 1, pp.75~82, 1998.
- [21] G. Liu, L.E. Murr, C.–S. Niou, J.C. McClure and E.R. Vega, Microstructural aspects of the friction–stir welding of 6061–T6 aluminum, Scripta Materialia 37 (1997), pp. 355–361



## Acknowledgments

지나온 2년이라는 시간을 돌이켜 보면 너무도 짧게 느껴집니다. 이 짧은 기간이 너무나도 소중한 시간이었음을 돌이켜 보며 작은 결실에 대한 감사의 글을 올립니다.

이 짧은 기간 동안 항상 부족한 저를 놓지 않으시고 끝까지 자신감을 심어 주시며 아낌없는 사랑과 질책으로 학문의 길을 이끌어주신 방한서 지도교수님께 고개 숙여 깊은 감사의 말씀 올립니다. 또한, 항상 독려와 지도편달을 해주신 방희선 교수님과 논문심사와 아낌없는 조언 해주신 권영섭 교수님, 이귀주 교수님께 감사의 마음을 전합니다. 아울러 이처럼 중요한 시기를 놓치지 않고 배움의 길을 선택할 수 있게 발판을 마련해주신 김하식 교수님, 박종남 교수님께 감사드립니다.

그리고 2년동안 항상 가족같이 생활하고 큰 힘이 되어준 구조용접실험실의 선 후배님들께 고마움의 뜻을 전하고 싶습니다. 많은 조언과 격려를 해주신 노찬승 선배님께 감사드리며 실험실을 이끌고 후배들에게 아낌없이 조언해준 창식이형, 형 실험하느라 고생한 현종이, 항상 형 걱정해주는 현수 그리고 실험실에 밝은 미소로 웃음을 주는 정미누나, 동기인 준형이, 용혁이, 아울러 부족한 형 따라주며 도움을 준 동생들 계성, 세민, 기상, 두송, 주연, 정한, 인도에서 유학와서 공부하며 논문 번역에 도움을 준 Bijoy 모두들 고맙습니다. 그리고 실험하는데 밖에서 많은 도움을 준 친구 충호, 승철이형, 정호형님 고맙습니다.

끝으로, 항상 아들을 믿고 걱정해주시고 사랑해주시며 묵묵히 지켜봐 주신 아버님, 어머님 그리고 많은 격려와 도움을 준 누나들과 매형, 기쁠 때 힘들 때 항상 옆에서 힘이 되어주고 함께해준 사랑하는 여자 친구 해란, 따뜻한 마음으로 항상 반겨주시고 챙겨주신 여자 친구 어머님, 아버님, 란희 모두들 진심으로 사랑한다는 말과 함께 깊은 감사를 드립니다.

2009년 12월

전 근 홍 올림

## 저작물 이용 허락서

학 과	선박해양공학과	학 번	20087128	과 정	석사
성 명	한글: 전근홍 한문: 全根弘 영문: JEON GEUN-HONG				
주 소	광주광역시 동구 학동 873-32				
연락처	E-MAIL : jgh71004008@lycos.co.kr				
논문제목	한글 : TIG-FSW Hybrid 용접기술을 이용한 이종재료 Al6061 Alloy - STS 용접부의 용접성에 관한 고찰. 영어 : A Study on Weldability of TIG Assisted Friction Stir Dissimilar Welding of Al6061 Alloy and STS Sheet.				

본인이 저작한 위의 저작물에 대하여 다음과 같은 조건아래 조선대학교가 저작물을 이용할 수 있도록 허락하고 동의합니다.

- 다 음 -

1. 저작물의 DB구축 및 인터넷을 포함한 정보통신망에의 공개를 위한 저작물의 복제, 기억장치에의 저장, 전송 등을 허락함
2. 위의 목적을 위하여 필요한 범위 내에서의 편집·형식상의 변경을 허락함. 다만, 저작물의 내용변경은 금지함.
3. 배포·전송된 저작물의 영리적 목적을 위한 복제, 저장, 전송 등은 금지함.
4. 저작물에 대한 이용기간은 5년으로 하고, 기간종료 3개월 이내에 별도의 의사 표시가 없을 경우에는 저작물의 이용기간을 계속 연장함.
5. 해당 저작물의 저작권을 타인에게 양도하거나 또는 출판을 허락을 하였을 경우에는 1개월 이내에 대학에 이를 통보함.
6. 조선대학교는 저작물의 이용허락 이후 해당 저작물로 인하여 발생하는 타인에 의한 권리 침해에 대하여 일체의 법적 책임을 지지 않음
7. 소속대학의 협정기관에 저작물의 제공 및 인터넷 등 정보통신망을 이용한 저작물의 전송·출력을 허락함.

동의여부 : 동의( O ) 반대( )

2010 년 2 월

저작자: 전 근 홍 (서명 또는 인)

조선대학교 총장 귀하